

Acoustic anomalies at phase transformation to quasi-2D proton glass state in $\text{Cs}_5\text{H}_3(\text{SO}_4)_4 \times x\text{H}_2\text{O}$ crystal

S N Gvasaliya¹, A I Fedoseev¹, S G Lushnikov¹, V H Schmidt²,
G F Tuthill² and L A Shuvalov³

¹ Ioffe Physico-Technical Institute, 26 Polytekhnicheskaya Str., St Petersburg 194021, Russia

² Physics Department, Montana State University, Bozeman, MT 59717, USA

³ Institute of Crystallography RAS, 117333, Moscow, Russia

Received 20 September 2000, in final form 5 February 2001

Abstract

The paper describes Brillouin light scattering studies of longitudinal acoustic (LA) phonons in $\text{Cs}_5\text{H}_3(\text{SO}_4)_4 \times x\text{H}_2\text{O}$ (PCHS) crystals at temperatures from 100 K to 360 K. The acoustic response of the crystal at different frequencies is analysed in detail. It is shown that both the velocity and damping of sound exhibit a strong dispersion caused by relaxation processes in the region of transformation into the glass-like phase ($T_g \approx 260$ K). A strong anisotropy in the acoustic response, attributable to the quasi-two dimensional (quasi-2D) structure of PCHS, is revealed. The LA phonon damping is calculated in the framework of a number of relaxation models. It is shown that, in the vicinity of T_g , anomalies in ultrasonic damping of the LA phonons propagating in the basal plane reflect the cooperative effect of freezing of acid protons. At the same time, the anomaly in damping of the LA phonon propagating perpendicular to the basal plane is described in terms of the Debye model and is due to the interaction between protons on hydrogen bonds and LA phonons. This suggests that the proton glass state realized at $T < T_g$ is of quasi-2D nature.

1. Introduction

Partially disordered crystals are attracting ever-increasing attention from researchers since their physical properties can be controlled by intentional variation of the degree of disorder. This feature also makes them highly attractive for commercial use. Disordered crystals can be divided into compounds with static and dynamic disorder of one of crystal sublattices. Crystals with partial static disorder include different types of orientational glasses [1], spin glasses [2], relaxor ferroelectrics [3], etc. Dynamic disordering occurs, for instance, in superionic crystals [4]. Of particular interest in these materials are specific features of lattice dynamics, which are strongly affected by disorder. These include additional excitations (localized excitations, pseudo-spin modes, relaxation modes etc.) in the vibrational spectrum of the crystals and interaction of the additional excitations with phonons. It is difficult to obtain

a clear and self-consistent picture of the lattice dynamics of disordered materials, because this requires investigations in a wide frequency range. In particular, to analyse the behaviour of acoustic phonons, the whole set of modern experimental techniques should be used, from the internal friction method to inelastic neutron scattering, covering a frequency range of 13 orders of magnitude (from Hz to THz). This task is extremely complicated, and for this reason the behaviour of acoustic phonons at hyper- and ultrasonic frequencies is compared in most cases [1]. As a rule, even in such a limited frequency range, contributions from different processes leading to a considerable modification of the acoustic response of partially disordered crystals can be separated and identified [5].

Crystals of $\text{Cs}_5\text{H}_3(\text{SO}_4)_4 \times x\text{H}_2\text{O}$ (PCHS) belong to a new class of compounds with the general formula $\text{Me}_z\text{H}_y(\text{AO}_4)_{(z+y)/2} \times x\text{H}_2\text{O}$, where $\text{Me} = \text{Cs, Rb, NH}_4$; $\text{A} = \text{S, Se}$; $0 \leq x \leq 1$ [6]. A characteristic feature of the high-temperature phase of these crystals is the existence of a dynamically disordered network of hydrogen bonds responsible for a high protonic conductivity referred to as superprotonic [7, 8]. It has been shown experimentally that protons play a decisive role in the lattice dynamics of this class of compound. A strong isotope effect with respect to hydrogen manifests itself in a number of materials of the MeHAO_4 , $\text{Me}_3\text{H}(\text{AO}_4)_2$ and $\text{Me}_5\text{H}_3(\text{AO}_4)_4 \times n\text{H}_2\text{O}$ type as additional phases and structural phase transitions. This effect has been widely studied by various techniques (see, e.g., [9–11]). The protonic conductivity of PCHS is quasi-2D: $\sigma_a/\sigma_c \sim 50$, which means that the conductivity in the basal plane is nearly two orders of magnitude higher than that along the hexagonal axis [6]. This reflects a specific feature of the PCHS crystal structure formed by layers of SO_4 tetrahedra linked by hydrogen bonds and located in the basal plane. In fact, the quasi-2D dynamic network of hydrogen bonds, where the number of structurally equivalent positions for protons is three times as large as the number of protons themselves, is realized within this layer.

At room temperature, PCHS crystals belong to the hexagonal system with space group $\text{P6}_3/\text{mmc}$ ($a = 6.2455 \text{ \AA}$, $c = 29.690 \text{ \AA}$; $V = 1003 \text{ \AA}^3$; $Z = 2$) [12]. From the viewpoint of structural changes, events of particular interest occur in the vicinity of $T_{c1} = 414 \text{ K}$ and $T_{c2} = 360 \text{ K}$. At T_{c1} , a superprotonic phase transition accompanied by a symmetry change $\text{P6}/\text{mmm} \leftrightarrow \text{P6}_3/\text{mmc}$ occurs [12, 13], and at T_{c2} an isostructural phase transition associated with changes in the local symmetry of SO_4 tetrahedra takes place [14–16]. No other anomalies associated with the structure changes in protonic samples have been observed. With decreasing temperature, the dynamic disorder of the hydrogen bond network gives way to static disorder (both orientational and positional), and the transformation into a proton glass-like phase is realized in the vicinity of $T_g = 260 \text{ K}$ [17]. These features make the PCHS crystals unique objects for studying the effect of disorder on the physical properties of these materials.

The goal of this work was to study how the disordering affects the behaviour of longitudinal acoustic phonons at different frequencies by using the results of our Brillouin experiments and comparing them with the ultrasonic data reported in [18].

2. Experimental details

Colourless single crystals of PCHS were grown by slow evaporation from saturated water solution at room temperature. The obtained samples were in the form of plates with a developed basal plane and typical hexagonal facets. The crystal orientation was determined by using a polarizing microscope. A separate sample was used for each temperature cycle, and hence, all the single crystals used in our experiments had the same prehistory.

Light scattering spectra were taken using a single-mode Ar^+ Spectra-Physics laser with $\lambda = 488 \text{ nm}$. The laser radiation power was not higher than 50 mW. A backscattering geometry

was used. The scattered light was analysed by a three-pass piezoscanning Fabry–Perot interferometer with a Burleigh DAS-1 system with automatic signal acquisition and automatic alignment of the interferometer mirrors, which provided the finesse of the interferometer at $C = 50$. The measured free spectral range (FSR) of the interferometer varied within the limits 11–14 GHz.

For low-temperature measurements (294–120 K), an optical cryostat with sample cooled by a flow of nitrogen vapour was employed. The sample temperature was monitored with an accuracy of ± 0.1 K by two copper–constantan thermocouples in contact with the sample. For experiments at 294–420 K, a home-made optical furnace was used. The sample temperature was measured using a chromel thermocouple with an accuracy of ± 0.1 K.

The velocity (V) and damping (α) of longitudinal hypersonic phonons in the 180° scattering geometry were determined as

$$V = \frac{v\lambda}{2n} \quad (1)$$

$$\alpha = \frac{4\pi n\delta}{v\lambda} \quad (2)$$

where n is the refractive index of the crystal, v is the shift of the Brillouin component, and δ is its half width at half-maximum. In all calculations, we used the value $n = 1.51$ [19].

In this work, the temperature behaviour of longitudinal hypersonic phonons (LA) with $\mathbf{q}_{\text{ph}} \parallel c_h$ and $\mathbf{q}_{\text{ph}} \perp c_h$ (\mathbf{q}_{ph} is the acoustic phonon wave vector) in the PCHS crystals was studied. The LA phonon velocity in a hexagonal crystal is determined by the elastic moduli $C_{33} = \rho V^2$ for $\mathbf{q}_{\text{ph}} \parallel c_h$ and $C_{11} = \rho V^2$ for $\mathbf{q}_{\text{ph}} \perp c_h$, where ρ is the density of the crystal, taken from [12].

It was found to be more convenient to use relative changes in the velocity of hypersonic to analyse the data. Then we have from (1)

$$\frac{\Delta V}{V_0} = \frac{V(T) - V_0}{V_0} \approx \frac{v(T) - v_0}{v_0} \quad (3)$$

where V_0 and v_0 are the velocity and frequency of the hypersonic phonon shift at $T = 178$ K, respectively. This temperature was taken as reference for matching the data because at this point the disorder effects terminate at both ultra- and hypersonic frequencies. The approximate equality sign in (3) indicates that we do not take into account the temperature dependence of the refractive index in our calculations.

3. Behaviour of acoustic phonons

Figure 1 shows how the velocity of hypersonic LA phonons vary with temperature in the range 360 to 150 K. The behaviour of Brillouin light scattering above room temperature was discussed in detail in [16], and therefore we shall not consider here the high-temperature part of the temperature dependences. It should only be noted that we use a sufficiently wide temperature range to allow a correct treatment of the behaviour of hypersonic LA phonons in the PCHS crystals in the region of a transformation to the proton glass-like state. Indeed, it is evident from figure 1 that in the range from 330 to 290 K the temperature dependences of the hypersonic velocity in the crystals studied can be approximated by a linear function. Deviations from the linear temperature dependence start below 280 K, and a weak dispersion anomaly of velocity is observed at around T_g . At lower temperatures, beginning with $T \approx 235$ K, the experimental results are again well described by a linear temperature dependence, but with a smaller slope. This pattern is observed for phonons with both $\mathbf{q}_{\text{ph}} \parallel c_h$ and $\mathbf{q}_{\text{ph}} \perp c_h$. Thus, a weak anomaly

of the hypersonic velocity in the region of transformation into the glass-like phase extends for ~ 50 K and exists in all the experimental geometries discussed. This is due to a distribution of the relaxation times in the glass-like state, generally giving rise to dispersion anomalies in the acoustic phonon velocity. Simultaneously, the frequency dependence of acoustic anomalies must manifest itself [1, 5].

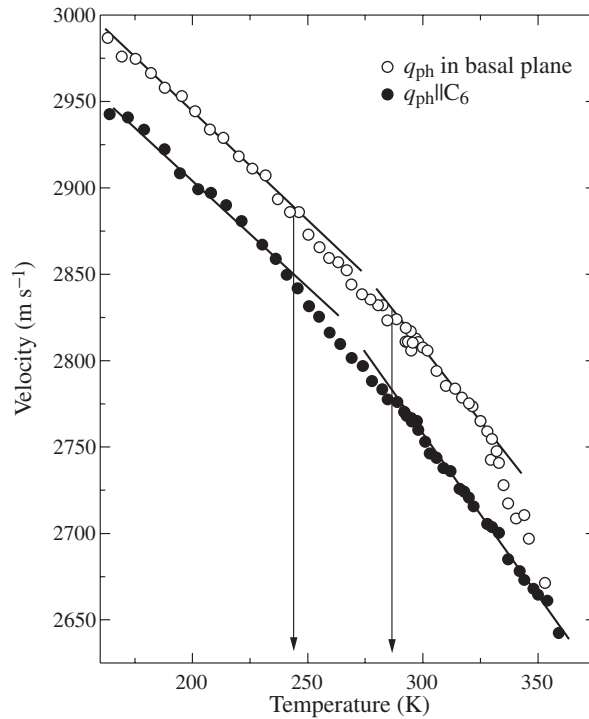


Figure 1. Temperature dependences of the velocity of longitudinal hypersonic acoustic phonons propagating in the basal plane and along the sixfold axis of the PCHS crystal. The arrows show the anomalous region in the vicinity of transformation into the proton glass state.

To study the behaviour of the acoustic response of a PCHS crystal at different frequencies, we compared the results obtained in our Brillouin light scattering experiments (i.e. at frequencies of the order of 10^{10} Hz) with the data furnished by ultrasonic measurements at frequencies of the order of 10^7 Hz [18]. Figures 2(a) and 2(b) show relative changes in the velocity of longitudinal acoustic phonons propagating in the basal plane and along the C_6 axis at ultrasonic and hypersonic frequencies. As a reference point of the temperature dependences, temperatures near $T = 178$ K were taken. As seen from figures 2(a) and 2(b), the temperature dependences of velocity can be approximated by a linear function beginning with ~ 230 K. This gives grounds to suppose that the relaxation processes which are considerably affecting the behaviour of the LA phonon velocity terminate at $T \sim 200$ K, and at lower temperatures the temperature dependences of velocity are governed by the lattice anharmonicity alone. Therefore, the use of the temperature mentioned above as a reference point in comparison with temperature dependences is justified.

Let us consider the behaviour of the LA phonon velocity at different frequencies. The first feature to be noted is a strong dispersion reflecting the frequency dependence of the relaxation contribution to the LA phonon velocity. Indeed, a decrease in the frequency at

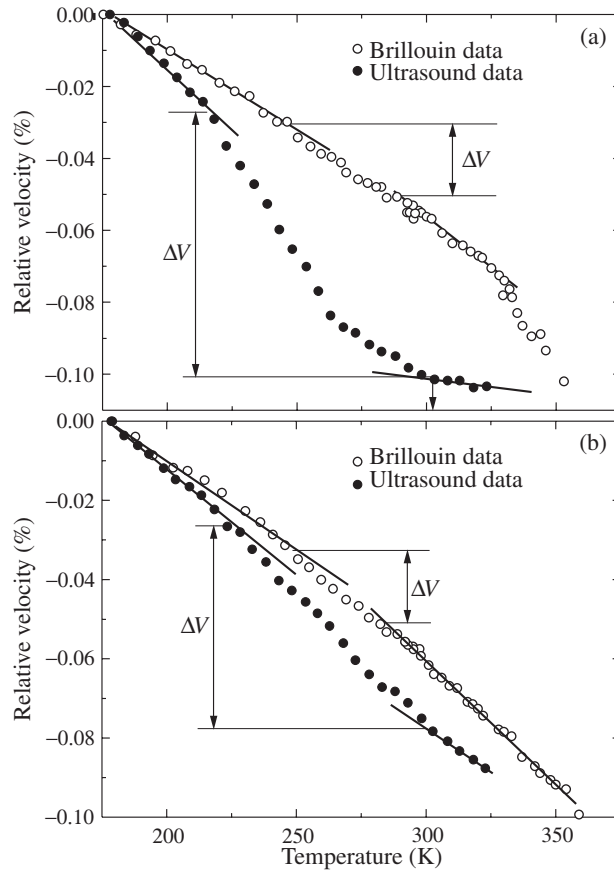


Figure 2. (a) Relative changes in LA phonon velocity in PCHS at ultra- and hypersonic frequencies versus temperature for $q_{\text{ph}} \perp c_h$ and (b) $q_{\text{ph}} \parallel c_h$. ΔV is the velocity jump (see the text). The ultrasonic data are taken from [18].

which the experiment is carried out (the probe frequency) leads to extension of the dispersion region associated with the logarithmic distribution of relaxation times. As a consequence, the velocity anomalies in ultrasonic measurements are significantly modified compared with the Brillouin frequencies. This accounts for the extension of the dispersion region from ~ 50 to 100 K and a fourfold increase (from 2% to 8%) in the velocity variation ΔV in the vicinity of T_g (see figures 2(a) and (b)). This means that a decrease in the probe frequency increases the value of the changes in the acoustic phonon velocity. This trend is well known from analyses of the behaviour of the acoustic response in the region of transformation into the glass-like phase of such compounds as $(\text{KBr})_{0.8}(\text{KCN})_{0.2}$ or $(\text{NaCN})_{1-x}(\text{KCN})_x$ [1] or in the vicinity of a diffuse phase transition in a relaxor ferroelectric $\text{PbMg}_{1/3}\text{Nb}_{2/3}\text{O}_3$ [20]. It should be noted that the changes in the LA phonon velocity in the PCHS crystal exhibit a strong dependence not only on frequency, but also on the phonon propagation direction. At ultrasonic frequencies, $\Delta V \sim 8\%$ for $q_{\text{ph}} \perp C_6$ and 5% for $q_{\text{ph}} \parallel C_6$. At hypersonic frequencies, the value of the velocity variation is nearly independent of the propagation direction and is equal to $\sim 2\%$. This is likely to be due to the participation of different relaxation mechanisms: at ultrasonic frequencies the velocity dispersion is mainly determined by the ‘slow’ α -relaxation, which is anisotropic, and the behaviour of hypersonic phonons is governed by the ‘fast’ isotropic β -relaxation. This

situation is widely discussed in the context of the mode-coupling theory, successfully used to describe the results obtained in studying the acoustic response in polymers [21] and glasses [22] at phase transformations.

Unfortunately, no theoretical model allowing a quantitative analysis of the effect of different processes on the sound velocity behaviour in the PCHS crystal has been suggested yet. For this reason we shall discuss the sound velocity behaviour on the qualitative level. Let us pay attention once more to the shape of the anomaly. In conventional orientational glasses the velocity has its local minimum in the vicinity of T_g . With decreasing probe frequency, the minimum becomes deeper and shifts towards lower temperatures [1]. For the PCHS crystal, the shape of the velocity anomaly is likely to be associated with a transition into the superionic phase, as, e.g., in Ag_2HgI_4 [23] or PbF_2 [24] crystals, or with transformation into the glass-like state, as in polymers [21] and some other materials in which relaxation anomalies with strong frequency dependence are observed in the temperature dependence of the acoustic phonon velocity [25].

Thus, anomalies in the velocity of sound in PCHS do not resemble those observed in 'classical' transitions into the orientational glass state. This is probably due to the fact that the lattice dynamics of PCHS do not contain a critical contribution from the structural phase transition, modified, e.g., by interacting ferro- and antiferroelectric order parameters, as in RADP, or by a translational-rotational interaction, as in quadrupolar glasses. The point is that the glass-like phase is formed in the majority of well known orientational glasses by competing interaction, which is absent, in its commonly accepted meaning, in the PCHS crystals.

3.1. Damping anomalies and differences between the behaviour of hyper- and ultrasonic phonons

The anomalies of the acoustic phonon velocity in the region of transformation of the PCHS crystal into the glass-like phase must have corresponding damping anomalies. Figure 3 shows the temperature dependences of the damping of hypersonic LA phonons with the polarization vectors q directed along the sixfold axis and lying in the basal plane, taken in the range 120 to 360 K. It is easily seen that the damping of hypersonic LA phonons does not exhibit any anomalies in the vicinity of T_g . A significant increase in damping of the phonon with $q_{\text{ph}} \perp C_6$ occurs only at $T \geq 320$ K and extends to 360 K, while for the phonon with $q_{\text{ph}} \parallel C_6$ the damping grows immediately in the vicinity of 360 K [16]. Above 360 K no Brillouin component could be detected in the light scattering spectra. A similar behaviour of light scattering was observed in Raman experiments, where the background and the contribution of quasi-elastic scattering sharply increased in the vicinity of $T = 360$ K [14], which points to considerable changes in the light scattering conditions in the crystal (formation of cracks, inhomogeneities etc.). In [16], damping anomalies in the vicinity of 360 K were attributed to an isostructural phase transition.

The behaviour of LA phonons at ultrasonic frequencies [18] appreciably differs from our findings: a broad damping peak correlating with the velocity anomalies of the corresponding ultrasonic background is observed in the vicinity of T_g [18] (compare figures 3, 4 and 5). An analysis of the ultrasonic damping [18] revealed that the damping peak has relaxation nature and can be described in terms of a model with a Gaussian distribution of activation energies. It was quite natural to suppose that calculations relying on ultrasonic measurements would allow us to correctly describe the temperature evolution of damping of hypersonic LA phonons. Unfortunately, all attempts to reproduce the calculations made in [18] for ultrasonic frequencies and recalculate them to the Brillouin scattering results failed. For this reason we had to invoke a number of basic models used to analyse damping anomalies in partially disordered crystals.

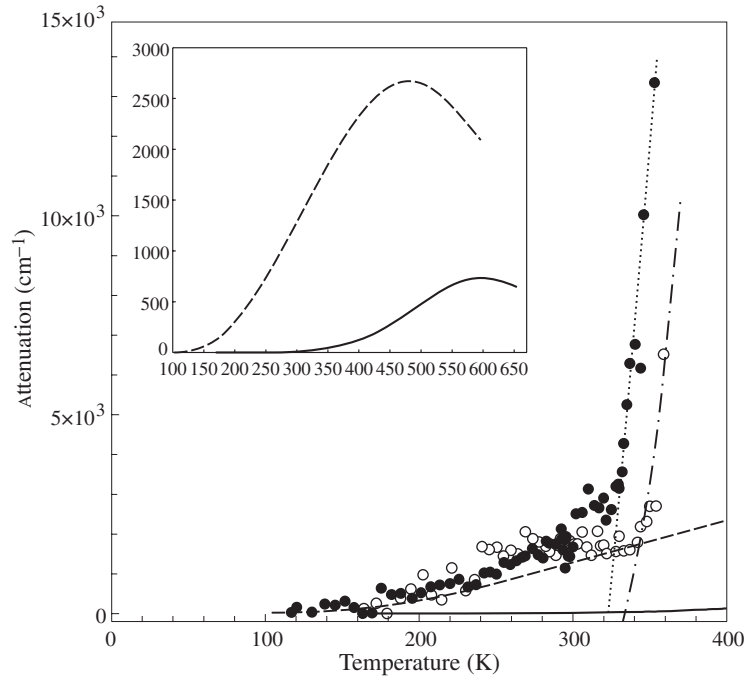


Figure 3. Temperature dependences of damping of longitudinal hypersonic acoustic phonons propagating in the basal plane and along the sixfold axis of the PCHS crystal. The full and broken curves show changes in damping at hypersonic frequencies recalculated from ultrasonic data. The dash-and-dot and dotted curves indicate the possible anomalous contribution of the isostructural phase transition to the damping. The inset presents the calculated relaxational hypersonic damping.

3.1.1. The relaxation mechanism in damping of acoustic phonons

Debye model. In a number of cases (low concentration of two-level systems, mobile atoms or ions) relaxation damping can be defined as a Debye-like process with a single relaxation time τ

$$\alpha = \frac{NB^2}{4\pi\rho v^3 kT} \omega \frac{\omega\tau}{1 + \omega^2\tau^2} \quad (4)$$

where N is the number of mobile atoms or ions, B is the deformation potential constant and k is the Boltzmann constant. It is assumed that the relaxing units are identical and interact with the deformation field independently of one another. It is evident that in this case the damping peak occurs at $\omega\tau \sim 1$.

Model with distribution of activation energies. However, there are many situations when the relaxation damping contour is much broader than the classical Debye contour, which means that the curve cannot be described in terms of the model with a single relaxation time. A conventional approach to resolve this difficulty, successfully applied to a large number of compounds (see, e.g., [26–30]), is as follows: the observed damping is regarded as a sum of several Debye peaks corresponding to a distribution of activation energies (and, hence, a distribution of relaxation times). It is assumed that each Debye relaxator interacts with the deformation field independently. In this case the damping is given by

$$\alpha = \frac{NB^2}{4\pi\rho kT v^3} \omega \int \frac{g(E)\omega\tau(E)}{1 + \omega^2\tau(E)^2} dE \quad (5)$$

where the parameters of the distribution function $g(E)$ can be obtained by fitting the model to the experimental curve. Most often, the Gaussian distribution function is used

$$g(E) = \frac{1}{\sqrt{2\pi} E_0} \exp \left[-\frac{(E - E_a)^2}{2E_0^2} \right] \quad (6)$$

where E_a is the activation energy for overcoming the barrier separating two potential minima, and E_0 is the dispersion of the Gaussian distribution (in the given case it corresponds to the activation energy range for ions interacting with the deformation field).

Universal model. In superionic conductors the concentration of mobile ions is fairly high and the assumption that relaxators are independent can prove physically unjustified. In this situation it would be expected that the relaxing system will exhibit a pronounced cooperative behaviour. In this case the temperature dependence of damping is adequately described by [27, 30]

$$\alpha \propto \frac{1}{T} \omega \frac{(\omega\tau)^m}{1 + (\omega\tau)^{1+m-n}} \quad (7)$$

where $0 \leq m, n \leq 1$. The maximum damping is reached at $\omega\tau = (m/(1-n))^{1/1-n+m}$. Note that at $m = 1$ and $n = 0$ the damping contour described by (7) will acquire a classical Debye shape. This means that the Debye model is a particular case of the universal model.

In all of the cases considered above it is assumed that the temperature dependence of the relaxation time has a thermal activation character and obeys the Arrhenius law [4]

$$\tau = \tau_0 \exp \left(\frac{E_a}{kt} \right) \quad (8)$$

where E_a is the activation energy, and τ_0^{-1} is the frequency of ion hopping between energetically equivalent positions (in the approximation of the absolute rate theory).

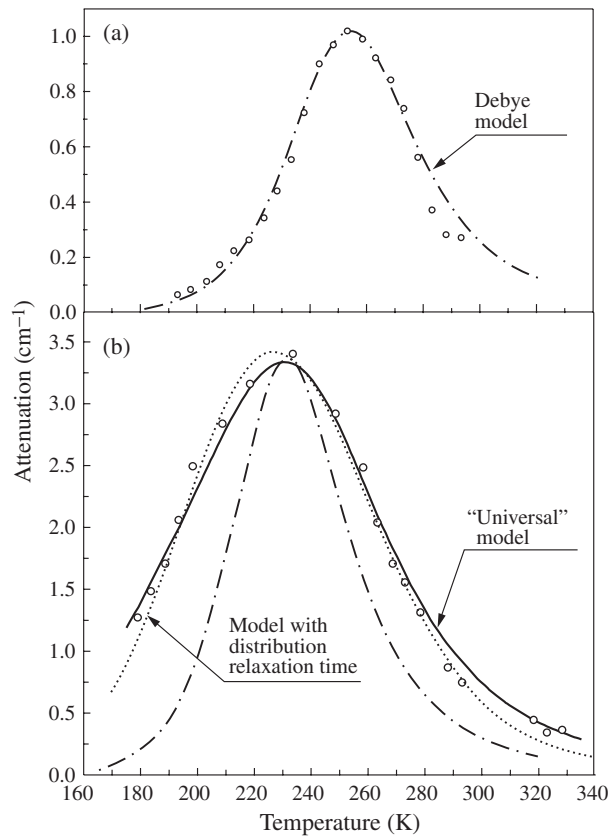
Having outlined the approaches used, we now discuss the results obtained.

3.1.2. Fitting and results Figure 4 presents the results of calculations relying on the classical Debye model (4) for the case of damping of ultrasound propagating along the sixfold axis (the [001] direction). It is easily seen that the data obtained using the model with a single relaxation time are in excellent agreement with experiment (standard deviation 0.04) for all temperatures. For protons located in the two-minimum potential of the hydrogen bond lying along the hexagonal axis, $\tau_0 = 4.8 \times 10^{-14}$ s, $E_a = 0.28$ eV (table 1). Recall that the Debye model is a particular case of the model with a relaxation time distribution (5) for $g(E)$ in the form of the Dirac delta function. By approximating the temperature dependence of damping in terms of the model with a distribution of activation energies, the authors of [18] obtained a very low activation energy dispersion $E_0 = 0.008$ eV corresponding, in principle, to the Dirac delta function ($E_0/E_a \sim 0.03$). Note that the activation energy obtained in our calculations coincides with the data of [18], although the relaxation time differs by about an order of magnitude (see table 1). Thus we have succeeded in describing adequately in terms of the Debye model the damping of an ultrasonic LA phonon propagating along the hexagonal axis. In this case the damping is governed by the interaction of acoustic waves with individual protons on hydrogen bonds.

Figure 4(a) illustrates the relaxation damping of ultrasound propagating in the basal plane, calculated using the models discussed above. It is obvious that the Debye model fails to describe adequately the observed damping contour (figure 4(b) shows the best fitting results with relaxation time and activation energy $\tau_0 = 4.8 \times 10^{-14}$ s and $E_a = 0.255$ eV). A more complicated pattern was obtained in calculations using the model with a Gaussian distribution

Table 1. Comparison of the model parameters from the present paper and from the existing literature.

Source	Direction	τ_0 (s)	E_a (eV)
This article	[001]	4.8×10^{-14}	0.28
	[100] ^a	4.8×10^{-14}	0.27
Reference [18]	[001] ^b	8.0×10^{-15}	0.32
	[100] ^c	8.0×10^{-15}	0.28
Reference [31]	—	1.0×10^{-12}	0.34
Reference [32]	—	8.7×10^{-14}	0.26
Reference [17]	—	8.0×10^{-15}	0.27

^a $m = 0.85$, $n = 0.65$ ^b $E_0 = 0.008$ eV^c $E_0 = 0.034$ eV**Figure 4.** Damping of ultrasonic LA phonon: (a) $q_{\text{ph}} \parallel c_h$ and (b) $q_{\text{ph}} \perp c_h$. Full circles represent experimental data [18], the dash-and-dot curve shows the results of our calculations in the framework of the classical Debye model (4); dots correspond to a calculation using the model of the activation energy distribution (5); and the full curve indicates our calculations in terms of the universal model (7).

of activation energies (5). Good agreement between the model and experiment (shown by dots in figure 4(b)) was found only for $\tau_0 = 1.5 \times 10^{-15}$ s, $E_a = 0.32$ eV, $E_0 = 0.057$, which, in our opinion, are not physically meaningful in this case: the relaxation time is too short and

the dispersion of E_a is rather large. Note that, to achieve consistency between the model (5) and experiment, expression (5) is to be integrated in the interval $6E_0$. The physical reason for such a wide range of activation energies for individual relaxators is unclear.

Only calculations in terms of the universal model gave excellent agreement (standard deviation 0.14) with the experimental temperature dependence of the damping curve for the acoustic phonon at ultrasonic frequency (figure 5). The parameters used in calculations with the model described by (7) were as follows: $\tau_0 = 4.8 \times 10^{-14}$ s, $E_a = 0.27$ eV, $m = 0.85$ and $n = 0.65$. With these parameters for m , n and τ_0 , the temperature at which the attenuation is at a maximum for the universal model, given by the condition $\omega\tau = (m/(1-n))^{1/1-n+m}$, should be about 94% of that for the Debye model with the same E_a and τ_0 . In fact, comparison of figures 4(a) and 4(b) shows that the ratio of the temperatures at which attenuation peaks are observed is approximately 0.92, lending support to our use of the different models to describe the attenuation of phonons propagating within, and perpendicular to, the basal plane.

Thus, in the basal plane, where the number of protons in energetically equivalent positions is much larger than in the hexagonal axis direction, damping is governed by the collective behaviour of the proton system. Note that the relaxation times and activation energies (i.e., the parameters that immediately determine the relaxator properties) obtained in our calculations are nearly the same for the [100] and [001] directions. In our opinion, this demonstrates that we have properly chosen the models, because it is quite reasonable to expect that parameters of the two-minimum potential do not depend appreciably on the crystallographic direction.

4. Discussion

We obtained parameters of the phenomenological models adequately describing ultrasonic measurements. Let us calculate changes in the relaxation damping of an acoustic phonon at hypersonic frequencies by using the values of E_a and τ_0 obtained in section 3.3 and compare them with the dependences obtained in Brillouin scattering experiments. Figure 3 shows experimental and theoretical temperature dependences of the hypersonic damping. The theoretical (calculated, to be more exact) damping dependences are the dependences recalculated from ultra- to hypersonic frequencies. In the vicinity of T_g , the calculated changes in damping at hypersonic frequencies correlate with our experiments. Above room temperature, the behaviour of the hypersonic damping is much more complicated: a sharp rise in damping is observed experimentally in the region of $T > 320$ K, absent in the calculated temperature dependences. Anomalies in the acoustic response of the crystal in the region of an isostructural phase transition T_{c2} [16] may contribute to hypersound damping in the vicinity of 360 K in addition to the calculated relaxational damping. Therefore, according to our calculations, the relaxation damping peak observed in the region of 250 K at ultrasonic frequencies is reached at hypersonic frequencies only at 480 K (see the inset of figure 3). In fact, this temperature cannot be attained since the PCHS crystal starts to decompose above 430 K.

Let us compare the τ_0 and E_a values obtained in our work with the results of other measurements (for illustrative purposes, the data are summarized in table 1).

NMR data for a powder sample of PCHS, differing from our results, were reported in [31] (see table 1). A probable reason for the discrepancy is, as stated by the authors of [31], 'a rough estimate of the results in the one-relaxation-time approximation', on the one hand, and an averaged estimate obtained in measurements on polycrystalline samples, on the other. Comparison of our data with those obtained in dielectric studies of the PCHS crystal [17, 32] gives more optimistic results. As seen from table 1, the activation energies obtained in dielectric measurements are similar to ours. The situation with the relaxation time is more complicated.

Thus, the activation energies and relaxation times obtained in our calculation correlate, on the whole, with the data of dielectric measurements of PCHS.

Let us return to our calculations in the preceding section. It was shown that the mechanism of the LA phonon damping at ultrasonic frequency in the vicinity of T_g strongly depends on the crystallographic direction. For an ultrasonic acoustic phonon propagating along the hexagonal axis, the damping is described by the classical Debye model. For damping of ultrasonic acoustic phonons propagating in the basal plane, the result is quite different: the anomaly in the vicinity of T_g is described with a good approximation in the framework of a phenomenological universal model involving a cooperative behaviour of protons. The situation when the relaxation in a crystal is governed by individual identical Debye relaxators in one direction, and by cooperative behaviour of relaxators in another, is surprising. To our knowledge, no situation of this kind has been described. This contradiction can be overcome if we suppose that a quasi-2D proton glass state is realized in the PCHS crystal below T_g . This means that the processes involved in the lattice dynamics of PCHS and associated with ‘freezing’ are pronounced in the basal plane and negligibly weak along the hexagonal axis. The suggested pattern corresponds to structural features of the PCHS crystal: the quasi-2D nature of the dynamically disordered network of hydrogen bonds is preserved at and below the freezing temperature. These processes are also reflected in α -relaxation anisotropy, revealed in analysis of the dielectric response dispersion of PCHS [17]. At the moment it can be supposed that the key role in the lattice dynamics is played by dipoles formed by random orientation of complexes consisting of SO_4 groups and protons connecting them in the basal plane of the PCHS crystal. Thus, we have obtained conclusive evidence that the proton glass state in the PCHS crystal can be defined as a quasi-2D system, or quasi-2D proton glass.

5. Conclusions

We have carried out Brillouin light scattering studies of the behaviour of longitudinal acoustic phonons in the PCHS crystal in a wide temperature range including the region of transformation into the glass-like state. Analysis involving comparison of the results obtained in studying the acoustics properties of the PCTS crystal at hypersonic ($f \sim 17$ GHz) and ultrasonic ($f \sim 10$ MHz) frequencies has revealed a number of exciting features. These are the dispersion of the velocity anomalies of acoustic phonons in the region of phase transformation into the glass-like state and the unusual anisotropy of damping anomalies at low (ultrasonic) frequencies. Temperature dependences of LA phonon damping drastically differ at different frequencies: a well-defined damping peak is present in the vicinity of T_g at ultrasonic frequencies and absent at hypersonic frequencies. In calculations carried out in the framework of different models, the most probable mechanisms of mechanical relaxation in the main directions, i.e., along the sixfold axis and in the basal plane, were revealed. It has been shown that the propagation of longitudinal sound along the C_6 axis can be described by the classical Debye model. It has been convincingly demonstrated that the sound damping in the basal plane is governed by the collective behaviour of protons located in energetically equivalent positions on hydrogen bonds.

Therefore, the proton glass state realized in the PCHS crystal at $T \leq 260$ K has a quasi-2D character. The dielectric and structural specific features of PCHS, together with our data, allow PCHS to be regarded as a representative of a new class of crystals in the quasi-2D proton glass-like state.

Acknowledgments

The authors wish to thank V V Dolbinina for sample growth. The work was supported by the Russian Foundation for Basic Research (Grant 99-02-18356) and National Science Foundation (Grant DMR-9805272).

References

- [1] Binder K and Reger J D 1992 *Adv. Phys.* **41** 547
- [2] Hochli U T, Knorr K and Loidl A 1990 *Adv. Phys.* **39** 405
- [3] GFisher K J and Hertz J A 1991 *Spin Glasses* (Cambridge: Cambridge University Press)
- [4] Siny I G, Lushnikov S G, Katiyar R S and Schmidt V H 1999 *Ferroelectrics* **226** 191
- [5] Boyce J B and Huberman B A 1979 *Phys. Rep.* **51** 191
- [6] Lynden-Bell R M and Michel K H 1994 *Rev. Mod. Phys.* **66** 721
- [7] Baranov A I, Kabanov O A, Merinov B V, Shuvalov L A and Dolbinina V V 1992 *Ferroelectrics* **127** 257
- [8] Merinov B V, Baranov A I, Shuvalov L A and Maksimov B A 1987 *Sov. Phys.-Crystallogr.* **32** 65
- [9] Abramic D, Dolinsek J, Blinc R and Shuvalov L A 1990 *Phys. Rev. B* **42** 442
- [10] Fukami T and Chen R H 1999 *Phys. Status Solidi b* **214** 219
- [11] Sumita M, Osaka T and Makita Y 1982 *J. Phys. Soc. Japan* **51** 1343
- [12] Lushnikov S G, Belushkin A V, Gvasaliya S N, Natkaniec I, Shuvalov L A, Smirnov L S and Dolbinina V V 2000 *Physica B* **276-278** 483
- [13] Merinov B V, Baranov A I, Shuvalov L A, Schneider J and Schulz H 1994 *Solid State Ion. Diffus. React.* **74** 53
- [14] Yuzyuk Yu I, Dmitriev V P, Loshkarev V V, Rabkin L M and Shuvalov L A 1995 *Ferroelectrics* **167** 53
- [15] Yuzyuk Yu I, Dmitriev V P, Loshkarev V V, Rabkin L M and Shuvalov L A 1994 *Crystallogr. Rep.* **39** 61
- [16] Lushnikov S G and Shuvalov L A 1999 *Crystallogr. Rep.* **44** 615
- [17] Lushnikov S G, Schmidt V H, Shuvalov L A and Dolbinina V V 2000 *Solid State Commun.* **113** 639
- [18] Baranov A I, Kabanov O A and Shuvalov L A 1993 *JETP Lett.* **58** 548
- [19] Yakushkin E D and Baranov A I 1997 *Phys. Solid State* **39** 77
- [20] Kadlec F, Yuzyuk Yu, Simon P, Pavel M, Lapsa K, Vanek P and Petzelt J 1996 *Ferroelectrics* **176** 179
- [21] Laiho R, Lushnikov S G and Siny I G 1992 *Ferroelectrics* **125** 493
- [22] Scheyer Y, Levelut C, Pelous J and Durand D 1998 *Phys. Rev. B* **57** 11212
- [23] Monaco G, Fioretto D, Masciovecchio C, Ruocco G and Sette F 1999 *Phys. Rev. Lett.* **82** 1776
- [24] Samulenis V I, Skritskii V L, Kezhenis A P, Mikuchenis V P, Orlyukas A S, Ermolenko Yu E and Glazunov S V 1987 *Sov. Phys. Solid State* **29** 1440
- [25] Catlow C R A, Harley R T and Hayes W 1978 *Brillouin Scattering and Lattice Defect Energetics of Superionics with the Fluorite Structure: Lattice Dynamics* ed M Balkanski (Paris: Flammarion Sciences)
- [26] Lushnikov S G and Shuvalov L A 1991 *Ferroelectrics* **124** 409
- [27] Esquinazi P and Koning R 1998 *Tunneling Systems in Amorphous and Crystalline Solids* ed P Esquinazi (New York: Springer)
- [28] Almond D P and West A R 1988 *Solid State Ion. Diffus. React.* **26** 265
- [29] Jackle J, Piche L, Arnold W and Hunklinger S 1976 *J. Non-Cryst. Solids* **20** 365
- [30] Borjesson L 1987 *Phys. Rev. B* **39** 4600
- [31] Almond D P and West A R 1981 *Phys. Rev. Lett.* **47** 431
- [32] Palmer R G, Stein D L, Abrahams E and Anderson P W 1984 *Phys. Rev. Lett.* **55** 958
- [33] Fajdiga-Bulat A M, Lahajnar G, Dolinsek J, Slak J, Lozar B, Zalar B, Shuvalov L A and Blinc R 1995 *Solid State Ion. Diffus. React.* **77** 101
- [34] Yuzyuk Yu, Dmitriev V, Rabkin L, Burmistrova L, Shuvalov L, Smutny F, Vanek P, Gregora I and Petzelt J 1995 *Solid State Ion. Diffus. React.* **77** 122